INFLUENCE OF DENSITY AND SURFACE/VOLUME RATIO ON THE COOLING RATE OF SINTER-HARDENING MATERIALS

G. F. Bocchini, A. Baggioli, B. Rivolta, G. Silva, P. Piccardo, E. Poggio

Abstract

A numerical approach has been adopted to investigate the influence of porosity and surface/volume ratio on the cooling rate of sinter-hardening steels. Parallelepipeds (rectangular prisms) of constant cross section and different heights were compacted at two different densities (6.8 and 7.0 g/cm^3) from a hybrid traditional diffusion-bonded powder and sintered at 1120°C, for 25 minutes, in industrial sinter-hardening equipment. During sintering and fast cooling periods, the temperature at the core of 25 mm height rectangular prism has been recorded. Through a mathematical approach, the heat transfer coefficients at the boundaries of the prism have been calculated from the experimental temperature values. Due to asymmetric flow during fast cooling in the sintering furnace, the boundary condition on the upper surface was considered to be different from the lateral and the lower surfaces. After specifying the boundary conditions, the direct problem has been formulated in order to calculate the temperature distribution as a function of time inside parallelepipeds characterized by different surface/volume ratios. These equations were solved using a commercial finite volumes numerical code. The results obtained show that the cooling rate depends on density: the higher the density, the lower the cooling rate, i.e. the influence of porosity on material hardenability is positive.

Keywords: alloy steels, hardenability, microstructural relationships, microstructure evolution, modeling, sinter hardening, thermal history

INTRODUCTION

The increasing application of sinter hardening requires a better knowledge of the cooling rate to be reached, not only on the part surface, to get the necessary hardness and strength. Since the internal cooling rate of parts having different geometry depends on the thermal conductivity of the constituting material and on the surface/volume ratio, a two-ways study has been carried out. In this first part of a more complete study, assuming that the thermal conductivity of PM steels is prevalently a simple function of material density only, the isothermal surfaces have been calculated by a numerical method. Two density values have been assumed: 6.8 and 7.0 g/cm^3. The analysis has been carried out on parallelepipeds of constant cross section and varying height. The possible mass ranges from about 200 grams to nearly 2 kg. It has been assumed that the cooling rates on the outer surfaces depend on cooling capacity of the equipment, i.e. on atmosphere flow-rate and temperature drop by external cooling, and on the orientation of the surface. The calculations allow getting a series of isothermal surfaces. For a given material hardenability, a certain

Gian Filippo Bocchini, Powder Metallurgy Consultant, Rapallo, Genova, Italy
Andrea Baggioli, Barbara Rivolta, Giuseppe Silva, Technical University, Lecco, Italy
Paolo Piccardo, Eleonora Poggio, University of Genova, Genova, Italy

isothermal surface should define the zones where different microstructures form upon cooling. In this preliminary study, any difference in diffusion of alloying additions, which could originate differences in local hardenability, has been neglected. The analysis of the results can help design engineers and parts manufacturers to find the optimum choice, especially for heavy and massive parts, among available materials. To confirm the indications obtained by the numerical approach, an experimental survey on part shapes like those analyzed by the numerical model has been carried out. The results and the global comparisons are described in another report.

MATERIALS AND METHODS

From a hybrid traditional diffusion-bonded powder (% Ni = 4.0; % Mo = 1.5; % Cu = 2.0) parallelepipeds of constant cross section and different heights have been pressed at two different densities: 6.8 and 7.0 g/cm^3 (0.6 % graphite in the mix). The samples have been sintered at 1120°C under endogas with carbon potential 0.6-0.7 %, 25 minutes soaking time, in industrial sinter-hardening equipment. During sintering and fast cooling periods, the temperature at the core of a 25 mm height parallelepiped has been recorded through a thermocouple.

Inverse Problem Solution

Through the knowledge of the temperature values at the core, the first step is to evaluate the heat transfer coefficients at the boundaries of the parallelepiped, which depend on the pattern of gas flow in the furnace and on the orientation of the surface.

The temperature distribution inside the parallelepipeds as a function of space and time is described by the following partial differential equation:

$$\rho_s \, c \frac{\partial T}{\partial t} = k_s \left(\frac{\partial^2 T}{\partial x^2} + \frac{\partial^2 T}{\partial y^2} + \frac{\partial^2 T}{\partial z^2} \right) \tag{1}$$

where: ρ_s is the density of the sintered material [kg m^{-3}],
c is the specific heat of the sintered material [J kg^{-1} K^{-1}],
k_s is the thermal conductivity of the sintered material [W m^{-1} K^{-1}],
T is the temperature [K],
t is the time [s].

The ratio $k_s/\rho\, c$ is the thermal diffusivity, [m^2 s^{-1}]. To evaluate the conductivity k_S of the sintered material, a well-known relation [1, 2] has been used:

$$k_s = k_{fd}(1-2\varepsilon) \tag{2}$$

where: k_{fd} is the conductivity of the fully dense material [W m^{-1} K^{-1}],
ε is the porosity of the sintered material.

The imposed boundary conditions are the following:

$$\dot{q} = h_i \left(T_s - T_\infty \right) \tag{3}$$

where: $\dot{q}$ = heat flux [W · m^{-2}]
h_i = heat transfer coefficient [W·m^{-2}·K^{-1}]
T_s = temperature of the surface [K]
T_∞ = free stream temperature [K]

The initial condition has been imposed as $T = T_0 = 1108$ K, while the free stream temperature has been considered equal to 333 K. Owing to the asymmetric flux during the fast cooling in the sintering furnace, the thermal exchange on the upper surface must be considered different from the lateral and the lower surfaces. That's why three different heat transfer coefficients must be considered: h_{up} for the upper surface, h_{lat} for the lateral surfaces and h_{low} for the lower surface, in contact with the belt of the furnace.

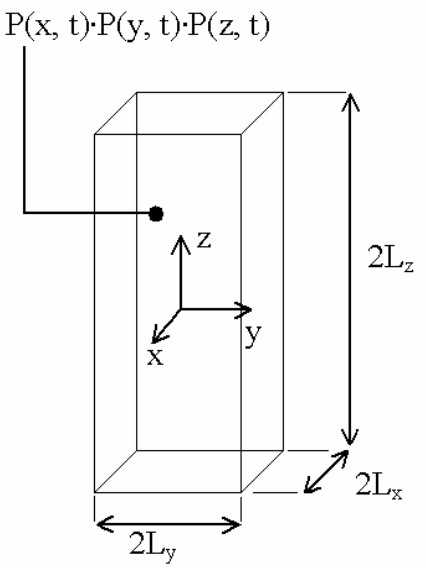

Fig.1. Schematic of the investigated geometry.

The temperature distribution in a parallelepiped can be calculated as the product of three one-dimensional solutions for the plane walls of thickness $2L_x$, $2L_y$ and $2L_z$ [3], according to the schematic representation in Fig.1. The solution can be expressed as:

$$\frac{T(x,y,z,t)-T_\infty}{T_0-T_\infty} = P(x,t)\cdot P(y,t)\cdot P(z,t) \qquad (4)$$

where the distances x, y, z are all measured with respect to a rectangular coordinate system whose origin is at the center of the parallelepiped. If we introduce the following dimensionless variables:

$$\theta_i = \frac{T_i - T_\infty}{T_0 - T_\infty} \quad x^* = \frac{x}{L_1} \quad y^* = \frac{y}{L_2} \quad z^* = \frac{z}{L_3}$$

$$Fo_i = \frac{k\,t}{\rho\, c\, {L_i}^2} \qquad Bi_i = \frac{h_i L_i}{k} \qquad \text{with i =1, 2, 3.}$$

the solution of (1) can be written as:

$$\frac{T(x,y,z,t)-T_\infty}{T_0-T_\infty} = \theta_1\cdot\theta_2\cdot\theta*_3 = C_1C_2\exp\left(-\zeta_1{}^2 Fo_1 - \zeta_2{}^2 Fo_2\right)\cdot\cos\left(\zeta_1 x^*\right)\cdot\cos\left(\xi_2 y^*\right)\cdot\theta_3^* \qquad (5)$$

ξ_i are the roots of the transcendent equation $\xi_i \tan \xi_i = Bi_i$; the coefficients C_i are calculated in function of ξ_i according to the following equation:

$$C_i = \frac{4 sin\, \zeta_i}{2\zeta_i + sin(2\zeta_i)} \tag{6}$$

with $i = 1, 2$.

θ^*_3 is the solution relative to the asymmetry of the heat transfer coefficients from the upper to the lower surface.

With regard to θ^*_3:

$$C_{3up} \exp\left(-\xi_3^{\,2} Fo_{3up}\right)\cos\left(\xi_3 z^*\right) \quad \text{if } z > z_{ad} \tag{7}$$

$$\theta^*_3 =$$

$$C_{3low} \exp\left(-\xi_3^{\,2} Fo_{3low}\right)\cos\left(\xi_3 z^*\right) \quad \text{if } z < z_{ad} \tag{8}$$

where:
$$C_{3up} = \frac{4 \sin \zeta_{3up}}{2\zeta_{3up} + \sin\left(2\zeta_{3up}\right)} \tag{9}$$

$$\xi_{3up} \tan \xi_{3up} = Bi_{3up} \tag{10}$$

$$Bi_{3up} = \frac{h_{3up} L_{3up}}{k} \tag{11}$$

$$L_{3\,up} = L_3 + z_{ad} \tag{12}$$

and

$$C_{3low} = \frac{4 sin\, \zeta_{3low}}{2\zeta_{3low} + sin\left(2\zeta_{3low}\right)} \tag{13}$$

$$\xi_{3low} \tan \xi_{3low} = Bi_{3low} \tag{14}$$

$$Bi_{3low} = \frac{h_{3low} L_{3low}}{k} \quad L_{3\,low} = L_3 - z_{ad} \tag{15}$$

z_{ad} is the distance of the adiabatic plane from the origin of the Cartesian coordinate system. The unknown variables of the so formulated inverse problem are: h_{lat}, h_{3low}, h_{3up} e z_{ad}. The thermo-physical properties c and k_{fd} of the sintered material are taken from literature, referring to a steel of similar chemical composition [4]. The specific heat c and the conductivity k_{fd} are considered temperature piece-linear functions [4].

To calculate the heat transfer coefficients, the total fast cooling time (20 minutes) has been divided into seven time intervals: each time interval is characterized by a constant cooling rate in the furnace. It must be considered that the knowledge of the cooling law at one point of a rectangular parallelepiped clearly means a mathematical indetermination system. That's why the evaluation of the heat transfer coefficients has been made with an iterative numerical method, which allowed to evaluate a number of heat transfer coefficients for every time interval. Among these coefficients, the only one characterized by the maximum difference between the upper and the lower heat transfer coefficients has been chosen. In this way, the most asymmetric cooling condition has been considered. The calculated heat transfer coefficients are shown in Tab.1.

Tab.1. Thermal exchange coefficients on the surfaces calculated solving the inverse problem.

Δt [min]	Heat transfer coefficients		
	upper	lateral [$Wm^{-2}K^{-1}$]	lower
0÷3	58	14	10
3÷5	110	30	20
5÷9	157	29	16
9÷11	112	29	16
11÷14	164	34	16
14÷16	109	20	10
16÷20	41	13	8

Direct Problem Solution

Considering the geometrical and thermal symmetry of the problem, the original model can be easily simplified as shown in Fig.2, where a difference with the original geometry can be easily detected.

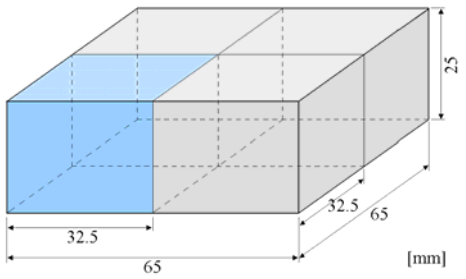

Fig.2. The simplified geometrical model: the difference with the original model can be easily detected.

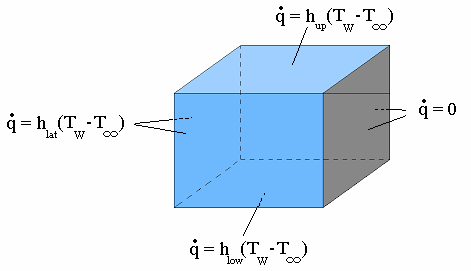

Fig.3. Schematic representation of the boundary conditions.

In order to calculate the temperature distribution in function of time, the boundary conditions for the equation (1) have been specified, as indicated in Fig.3.

As previously, the initial condition has been imposed at $T = T_0 = 1108$ K, while the free stream temperature T_∞ has been considered equal to 333 K. Numerical simulations have been made on specimens of heights equal to 25 mm, 40 mm and 63 mm to detect the influence of different ratios of surface/volume. The conductivity k_{fd} and the specific heat c have been taken from scientific literature, considering a steel of a similar chemical composition. We have also assumed that the behaviour of k_f and of c is piece-linear with temperature. The equation (1) with the boundary and initial conditions previously indicated has been solved using a commercial finite volumes numerical code (Fluent 5.5, Fluent Inc.). The spatial integration has been solved through a coupled method, while for the time integration, an implicit method has been used.

The quenching period has been considered equal to 20 minutes.

RESULTS

To detect the difference of temperature in the solid, four different points have been considered as shown in Fig.4, which represents a quarter of a complete sample. Figure 5 shows the transient temperature calculated in the 25 mm height parallelepiped.

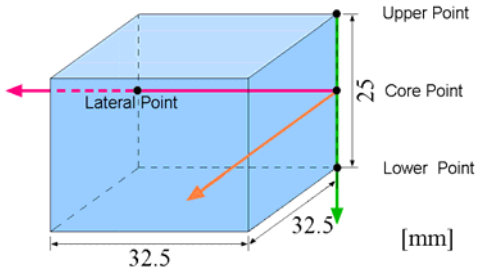

Fig.4. Geometrical element utilized for the study.

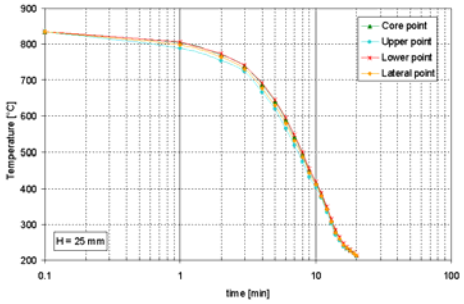

Fig.5. Temperature distribution in the parallelepiped with H = 25 mm.

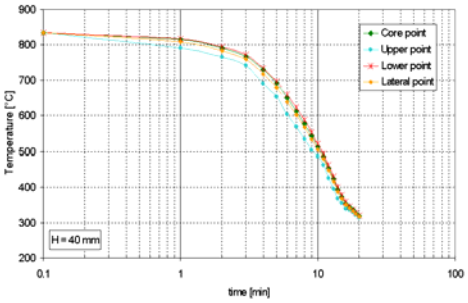

Fig.6. Temperature distribution in the parallelepiped with H = 40 mm.

ON THE POSSIBLE INFLUENCE OF DENSITY ON THERMAL DIFFUSIVITY

The various graphs show that the cooling rate, independently of the measurement or calculation point, depends on density. Astonishingly, the higher the density lower the cooling rate. The microstructure investigation, described in [4], confirms the results of the numerical evaluations. Moreover, Saritas, Doherty and Lawley [5] found, in an experimental way, a comparable result. Then it seems interesting to deepen this surprising result, achieved by different approaches and experimental methods.

The cooling rates at the core of the parallelepipeds 63 mm high, given by the curves of temperature versus time, are plotted in Fig.8. These curves have been drawn from the corresponding measured ones. To show more clearly the influence of density, the available data have been summarized in Fig.9, which shows with strong evidence, the influence of part density on the temperature reached at a certain time. To try to justify this apparently anomalous effect, it may be useful to analyze the formula that expresses the thermal diffusivity.

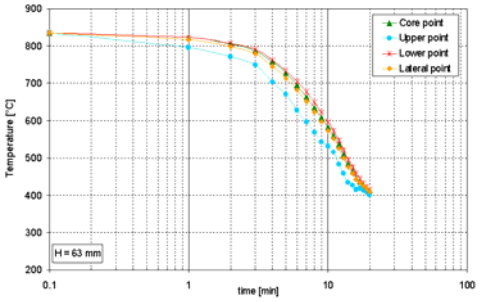

Fig.7. Temperature distribution in the parallelepiped with H = 63 mm.

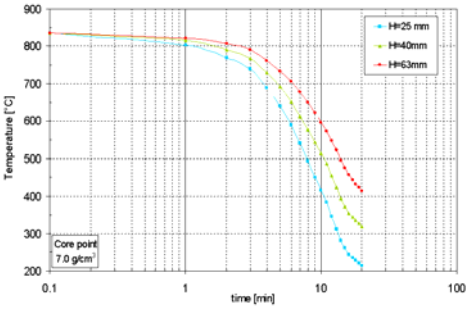

Fig.8. Temperature distribution at the core of parallelepipeds with various heights.

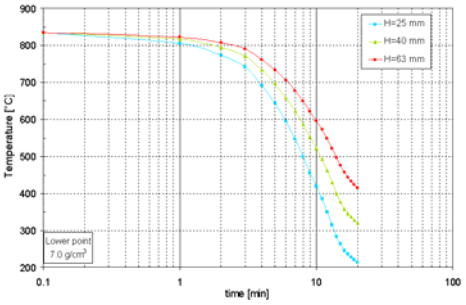

Fig.9. Temperature distribution at the bottom of parallelepipeds with various heights.

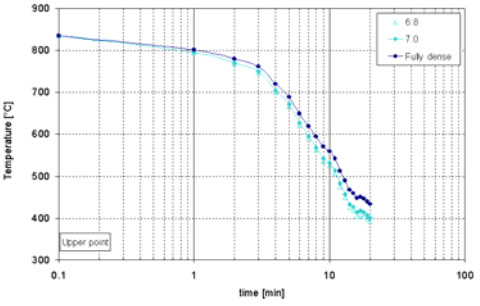

Fig.10. Influence of density on the temperature distribution at the upper face of 63 mm height parallelepipeds.

If each quantity is given as a function of porosity, we can write in the most general form

$$\frac{k_s}{\rho \cdot c_s} = \frac{k_0 \cdot (1 - A \cdot \varepsilon)}{\rho_0 \cdot (1-\varepsilon) \cdot c_0 \cdot (1-\varepsilon)} = \frac{k_0}{\rho_0 \cdot c_0} \cdot \frac{1 - A \cdot \varepsilon}{(1-\varepsilon)^2} \qquad (16)$$

where the subscript 0 indicates the fully dense steel, while the subscript s indicates the sintered steel.

Formula (4) shows that the thermal diffusivity of sintered steel is higher than that of equivalent fully dense steel if it is

$$1 - A \cdot \varepsilon > (1-\varepsilon)^2 \qquad (17)$$

namely if it is

$$A < 2 - \varepsilon \qquad (18)$$

This inequality does not appear completely incompatible with available experimental data. Just as an example, from the results plotted in Fig.14, if we consider the lowest temperature, it should be A = 1.6 to explain the experimental achievements. For better readability of data, in Figs.15 and 16 the hysocronic and isothermal curves at the core are plotted versus density on the investigated materials.

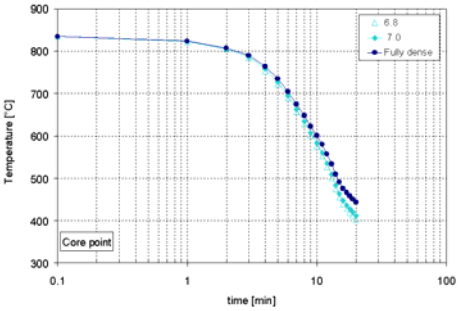

Fig.11. Influence of density on the temperature distribution at the core of 63 mm height parallelepipeds.

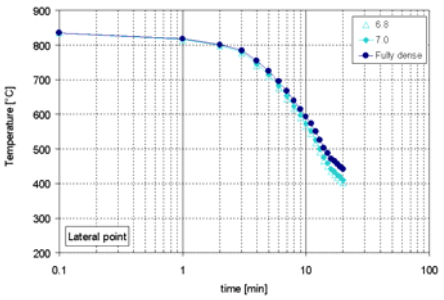

Fig.12. Influence of density on the temperature distribution at the sides of 63 mm height parallelepipeds.

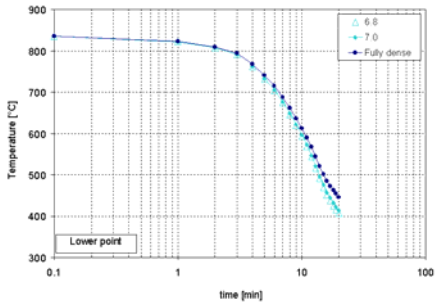

Fig.13. Influence of density on the temperature distribution at the bottom of 63 mm height parallelepipeds.

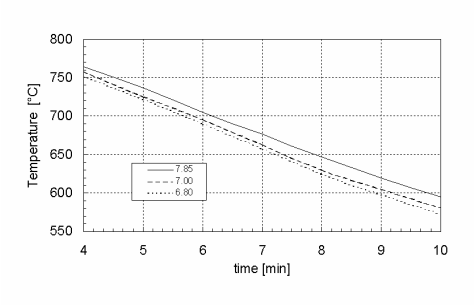

Fig.14. Curves of temperature versus time at different densities. Parallelepipeds with 63 mm height; core.

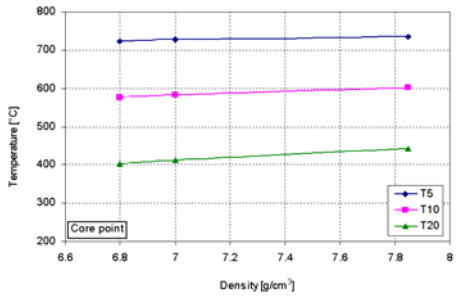

Fig.15 Curves of temperature versus density, after 5 (T5), 10 (T10) and 20 (T20) minutes. Core point in 63 mm height parallelepipeds.

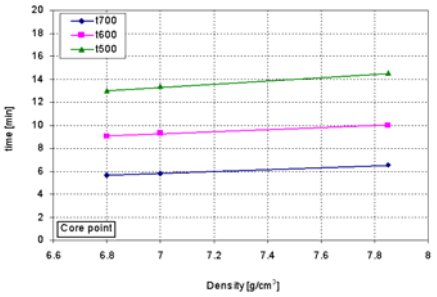

Fig.16. Curves of time versus density to reach 700°C (t700), 600°C (t600), 500°C (t500).

CONCLUDING REMARKS

Through temperature measurements on parallelepipeds during the fast cooling stage, inside a suitable sinter-hardening industrial furnace, heat transfer coefficients have been estimated. Through a commercial finite volume code, the temperature distributions in

function of time have been calculated inside parallelepipeds characterized by different surface/volume ratios. The calculated temperature profiles appear surprising: it seems that the cooling rate is not directly in proportion to density; on the contrary, the higher the porosity the higher the cooling rate.

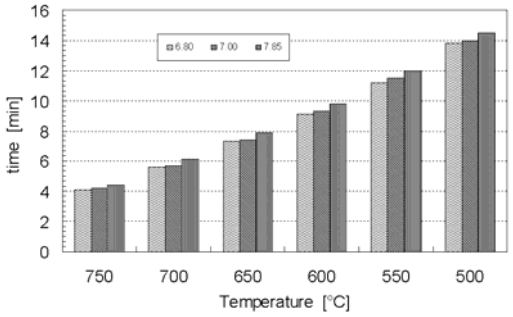

Fig.17. Influence of density on the times required to reach different temperatures on cooling from 835°C.

This apparent anomaly can be explained and justified analyzing the formula which gives us the thermal diffusivity of porous steels, and introducing the influences of porosity on physical properties [5, 6].

As to some discrepancies between the results published by Saritas et al., [7], and our results, the deviation of the solutions can be attributed to the convective boundary conditions. According to [3], if the model implies a trifling inner resistance, the solutions depend on the convective heat transfer coefficient, h, and on the heat capacity according to the simplified formula:

$$T = T_\infty + (T_0 - T_\infty)\, e^{-\frac{h}{\rho c L}t} \qquad (19)$$

where L is the ratio between volume and external surface.

Contrary to the common opinion, the investigation carried out showed that the influence of porosity on material hardenability is positive. Of course, when selecting material density for demanding applications, other properties, such as yield and ultimate tensile strength, macrohardness, reliability, risk of brittleness, rigidity, must be adequately considered.

Due to the observed influence of porosity, it will be interesting to explore a wider range of materials density, with a special attention focused on thermal conductivity, heat capacity, and thermal diffusivity.

Acknowledgements

The authors warmly thank the company Stame (Arosio, CO, Italy) for the care in preparing the samples for the present investigation.

REFERENCES

[1] Bocchini, GF.: Reviews on Powder Metallurgy and Physical Ceramics, 1983. Ed. M.B. Waldron. London : Freund Publishing House Ltd, 1983

[2] Bocchini, GF. In: Advances in P/M & Particulate Materials. Proc.Int.Con., New Orleans, MPIF, 2001

[3] Incropera, FP., DeWitt, DP.: Introduction to Heat transfer. John Wiley & Sons, 1996
[4] Smithells Metals Reference Book. 7th ed. E.A. Brandes & G.B.Brook, 1992
[5] Bocchini, GF., Ienco, MG., Rivolta, B., Silva, G., Stagno, E. In: 2002 World Congress on Powder Metallurgy & Particulate Materials, Orlando, June 16-21 2002
[6] Bocchini, GF., Baggioli, A., Gerosa, R., Rivolta, B., Silva, G.: accepted to be published on International Journal of Powder Metallurgy.
[7] Saritas, S., Doherty, RD., Lawley, A.: The International Journal of Powder Metallurgy, vol. 38, 2002, no.1, p. 31